PHYSICAL REVIEW B **89**, 060501(R) (2014)

# Hysteretic behavior in the optical response of the underdoped Fe-arsenide $Ba(Fe_{1-x}Co_x)_2As_2$ in the electronic nematic phase

C. Mirri,[1] A. Dusza,[1] S. Bastelberger,[1] J.-H. Chu,[2,3,4] H.-H. Kuo,[2,3,4] I. R. Fisher,[2,3,4] and L. Degiorgi[1,*]

[1]*Laboratorium für Festkörperphysik, ETH-Zürich, 8093 Zürich, Switzerland*

[2]*Stanford Institute for Materials and Energy Sciences, SLAC National Accelerator Laboratory, 2575 Sand Hill Road, Menlo Park, California 94025, USA*

[3]*Geballe Laboratory for Advanced Materials, Stanford University, Stanford, California 94305, USA*

[4]*Stanford Department of Applied Physics, Stanford University, Stanford, California 94305, USA*

(Received 31 October 2013; revised manuscript received 15 January 2014; published 7 February 2014)

We use a new technique that allows *in situ* variation of uniaxial stress to probe the polarization dependence of the optical reflectivity of the representative underdoped iron-arsenide $Ba(Fe_{1-x}Co_x)_2As_2$ through the tetragonal-to-orthorhombic structural transition and with respect to their electronic nematic phase. These measurements reveal a hysteretic behavior of the anisotropic optical response to uniaxial stress in the orthorhombic state associated with twin boundary motion, whereas the pressure-induced anisotropy of the optical response is reversible in the tetragonal state.

DOI: 10.1103/PhysRevB.89.060501 PACS number(s): 74.70.Xa, 64.70.M−, 78.20.−e

The parent phase of Fe-arsenide and chalcogenide superconductors harbors antiferromagnetic order with a critical temperature $T_N$. These materials also significantly undergo a structural phase transition that breaks the fourfold rotational symmetry of the tetragonal phase and either accompanies ($T_s = T_N$) or precedes ($T_s > T_N$) the onset of long range magnetic order [Fig. 1(a)] [1,2]. The physical origin of this effect remains a matter of debate, with suggestions spanning spin-driven nematic order, orbital order, a combination of both, and a Pomerancuk-type instability [3–9]. Understanding the origin and consequences of the structural phase transition is also an important component for testing tentative connections to the physics of other novel superconductors, such as the cuprates. A variety of experiments, including dc transport [10–15], thermopower [16], elastic shear modulus [17,18], neutron scattering [19–21], angle-resolved photoemission spectroscopy (ARPES) [22–24], optical reflectivity [25–28], Raman spectroscopy [29], and local probes such as scanning tunneling microscopy [30,31] and magnetic torque [32], have revealed a large electronic and magnetic anisotropy in the low-temperature orthorhombic phase, which argues for an electronically driven mechanism. More recently, elastoresistance measurements probing the response to uniaxial strain [11,15] in the high-temperature tetragonal state have exhibited the presence of a diverging nematic susceptibility, directly implying that the tetragonal-to-orthorhombic structural phase transition is indeed driven by some form of electronic nematic order.

Any phase transition that breaks a point group symmetry naturally leads to domain formation. A classic example is the case of an Ising ferromagnet, for which the spontaneous magnetization can point either up or down relative to the quantization axis; cooling such a material in zero field results in domain formation, which minimizes the magnetostatic energy. A related example is that of ferroelastic phase transitions. In the case of a tetragonal-to-orthorhombic transition, as exhibited by underdoped iron-arsenide superconductors, a spontaneous strain at low temperatures can be oriented in one of two possible directions, and a twin domain structure forms to minimize the elastic energy (Fig. 1) [1,2]. Just as a magnetic field $H$ couples to the magnetization $M$ of a ferromagnet, leading to the familiar $M(H)$ hysteresis behavior below and to the associated susceptibility above the Curie temperature, so does in-plane anisotropic biaxial strain couple to ferroelastic order (Fig. 1).

Here, we describe results of reflectivity measurements that probe the optical response to variable uniaxial stress for the prototypical underdoped iron-arsenide $Ba(Fe_{1-x}Co_x)_2As_2$. Optical reflectivity measurements present a rather unique perspective on the nematic order in these materials. In the low frequency ($\omega$) regime, such measurements can distinguish anisotropy in the spectral weight from anisotropic scattering [1,25–28]. Meanwhile, in the high frequency regime, of relevance to this Rapid Communication, the reflectivity probes electronic anisotropy at much larger energy scales. Our measurements reveal a hysteretic behavior of the anisotropic optical response associated with the domain-wall motion and clearly demonstrate that the electronic anisotropy associated with the orthorhombicity extends far from the Fermi energy, with implications for the mechanism responsible for the electronic nematic phase.

To enable the experiments described in this Rapid Communication, we have designed a novel pressure device, allowing us to perform optical reflectivity [$R(\omega)$] measurements as a function of temperature under a variable in-plane uniaxial stress, thus with an adjustable population of the two twin orientations. The device consists of a sealed spring bellows, which can be expanded or retracted by varying the pressure of the He gas held inside, so that uniaxial stress on the lateral edge of the specimen can be tuned *in situ*. Our as-grown single crystals were cut into rectangular pieces with the tetragonal $a$ axis oriented at 45° to the edges of the sample so that the direction of the applied stress lies parallel to the orthorhombic $a$ and $b$ axes. For compressive stress the shorter $b$ axis is preferentially aligned along the direction of the stress [Fig. 1(a)] [1]. The $R(\omega)$ spectra were collected with the

*Author to whom correspondence and requests for materials should be addressed: degiorgi@solid.phys.ethz.ch

 

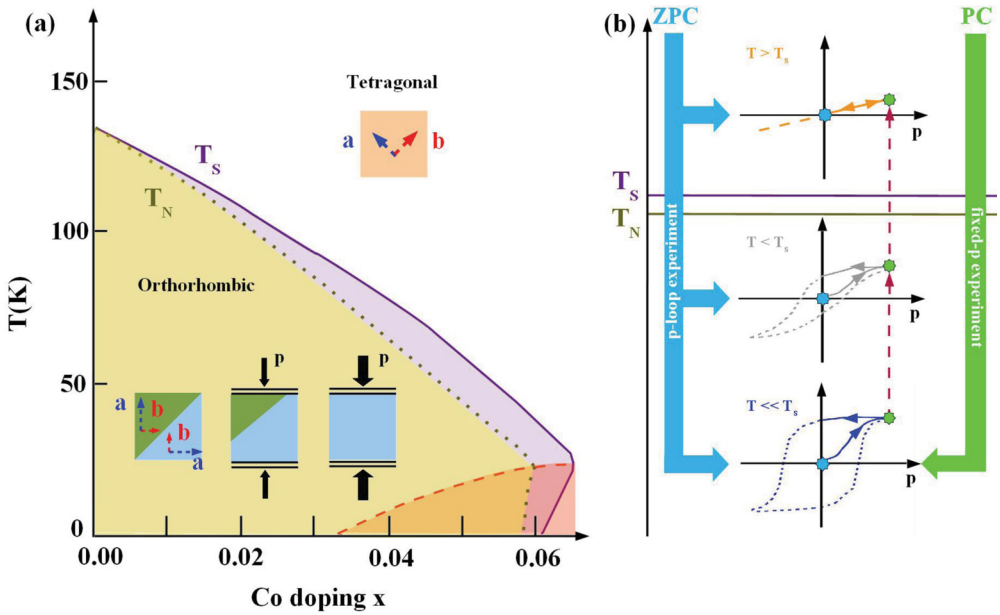


FIG. 1. (Color online) Ferroelastic tetragonal-to-orthorhombic structural transition in $Ba(Fe_{1-x}Co_x)_2As_2$: (a) Schematic phase diagram, emphasizing the underdoped regime. These materials tend to form dense structural twin domains as they are cooled through the ferroelastic tetragonal-to-orthorhombic transition at $T_s$. As illustrated schematically in the inset to (a), uniaxial pressure $p$ (black arrows) affects the relative population of twins oriented with the (elongated) $a$ axis parallel (green domain) and perpendicular (blue domain) to the applied stress. (b) illustrates two types of temperature and pressure cycles used for our experiments, which we refer to as zero-pressure-cooled (ZPC) pressure-loop experiments (blue arrows) and pressure-cooled (PC) fixed-$p$ experiments (green arrow), respectively. For the ZPC $p$-loop experiment the $p$ dependence of the optical anisotropy is measured following an initial cooling in zero pressure (blue stars). For the PC fixed-$p$ experiment, the sample is cooled to 10 K (i.e., $T \ll T_s$) at fixed $p$ and then the optical anisotropy (green stars) is collected upon warming at the same $p$ (dark-red arrows).

electromagnetic radiation polarized perpendicular or parallel to the applied stress (i.e., along the majority $a$ or $b$ axis), in the following defined as $R_a(\omega)$ and $R_b(\omega)$, respectively. Further details on the experimental technique can be found in the Supplemental Material (SM) in Ref. [33].

In this work we focus our attention on the midinfrared (MIR) spectral range, where a strong signature of the optical anisotropy was previously identified at approximately 1500 $cm^{-1}$ for detwinned $Ba(Fe_{1-x}Co_x)_2As_2$ crystals [25–28]. We report results obtained from (i) zero-pressure-cooled (ZPC) "pressure-loop" and (ii) pressure-cooled (PC) "fixed-pressure" experiments [Fig. 1(b)]. Applied stress is given in bars and corresponds to the pressure of the He gas inside the volume of the pressure device [33]. In (i) we reach the selected temperature ($T$) without applying pressure ($p$) and at that fixed $T$ we measure $R(\omega)$ at progressively increasing $p$ from 0 up to 0.8 bars. We subsequently collect $R(\omega)$ when releasing $p$ from 0.8 to 0 bars, thus completing the $p$ loop [Fig. 1(b)]. In (ii) at $T \gg T_s$ we apply $p = 0.3$ or 0.8 bars. At either fixed $p$ we cross the structural transition at $T_s$ and cool down to 10 K. At that constant $p$ we measure $R(\omega)$ with increasing $T$ from 10 K to well above $T_s$. Additional experimental protocols that corroborate our findings are given in Ref. [33].

Representative $R(\omega)$ data for the parent compound ($x = 0$, $T_s = T_N = 135$ K) are shown in Fig. 2(a) at 10 K and with $p = 0.8$ bars following an initial ZPC protocol. A comprehensive display of the $T$ and $p$ dependence of the measured MIR reflectivity for $x = 0$ as well as data pertaining to the $x = 2.5\%$ Co doping is presented in Ref. [33]. Anisotropy of $R(\omega)$ in the MIR [i.e., for $\omega \leqslant 3000$ $cm^{-1}$; see also the inset of Fig. 2(a)] between the two polarization directions is clearly visible in the raw data. In order to emphasize the evolution of the optical anisotropy as a function of pressure and temperature, we calculate the ratio $R_{\text{ratio}}(\omega) = R_a(\omega)/R_b(\omega)$. Figures 2(b)–2(g) show the $p$ dependence of $R_{\text{ratio}}(\omega)$ at 10, 120, and 140 K obtained from ZPC $p$-loop experiments. At 10 K (i.e., $T \ll T_s$) $R_{\text{ratio}}(\omega)$ is progressively enhanced when $p$ is increased and appears to saturate for $p \geqslant 0.6$ bars. At this temperature, the anisotropy is almost completely retained when $p$ is subsequently released back to 0 bars. At the higher temperature of 120 K the enhancement of $R_{\text{ratio}}(\omega)$ upon applying $p$ is smaller than that at 10 K, but drops to a smaller value when $p$ is released. By 140 K (i.e., $T > T_s$), the $p$ dependence of $R_{\text{ratio}}(\omega)$ is fully reversible so that the $p$-induced optical anisotropy is completely suppressed upon releasing $p$.

The deviation from isotropic behavior is best represented by the quantity $\Delta R_{\text{ratio}} = R_{\text{ratio}} - 1$ [34]. The $p$ dependence of $\Delta R_{\text{ratio}}$ at 1500 $cm^{-1}$ (dashed line in Fig. 2) for the ZPC $p$-loop measurements described above is shown in Fig. 3 for several representative temperatures. For temperatures $T < T_s$ we encounter a clear half hysteresis [Fig. 1(b)], reminiscent of the $M(H)$ behavior observed for a ferromagnet at $T < T_C$ ($T_C$ being the Curie temperature). The virgin curve, obtained after the initial ZPC, shows only a modest increase in $\Delta R_{\text{ratio}}$ for small $p$ (i.e., $p \leqslant 0.4$ bars), but the optical anisotropy rapidly grows for larger $p$ [Figs. 3(a)–3(d)]. As pointed out

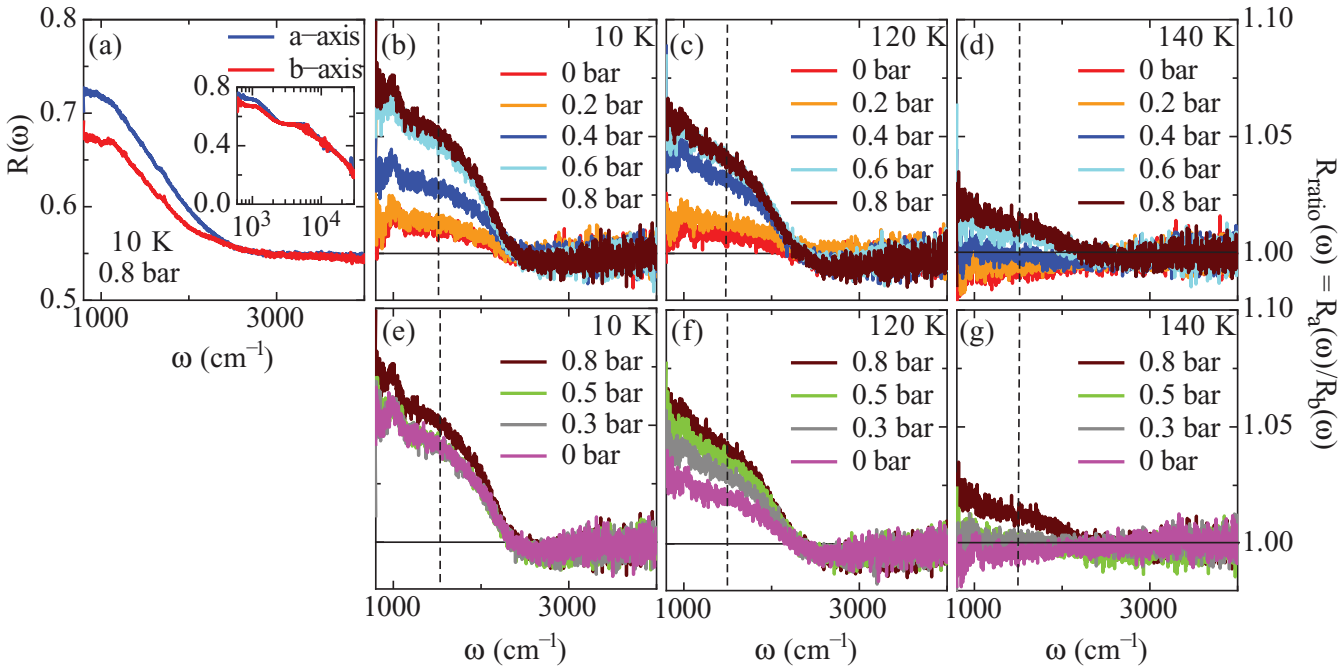


FIG. 2. (Color online) Representative data of the optical reflectivity of $BaFe_2As_2$ for the zero-pressure-cooled experiments: (a) Reflectivity [$R(\omega)$] measured at 10 K and $p = 0.8$ bars, displaying the optical anisotropy in the MIR spectral range. The inset shows $R(\omega)$ up to the visible and ultraviolet range with a logarithmic frequency scale. Above 3000 cm$^{-1}$ the spectra for both polarization directions merge together [33]. (b)–(g) $p$ dependence of $R_{\text{ratio}}(\omega)$ (see text) at 10, 120, and 140 K for increasing (b)–(d) and decreasing $p$ (e)–(g). Values of $R_{\text{ratio}}(\omega)$ (see text and Fig. 3) are determined at 1500 cm$^{-1}$ (vertical dashed line). Applied stress is given in bars and corresponds to $p$ of He gas inside the volume of the pressure device [33].

for the raw $R_{\text{ratio}}(\omega)$ data (Fig. 2), the optical anisotropy $\Delta R_{\text{ratio}}$ saturates for $p > 0.6$ bars at $T < T_s$. This saturation at $T \ll T_s$ presumably reflects complete detwinning of the sample, and any subsequent $p$ dependence arises from the intrinsic response to $p$ of the orthorhombic structure. By releasing $p$ back to 0 bars, the remanent optical anisotropy, due to the imbalance of the two twin orientations that remain frozen in place, can be probed. At 10 K, the material shows essentially no change in optical anisotropy as $p$ is reduced below 0.6 bars, indicating that the sample remains in a single domain state. In this case, $\Delta R_{\text{ratio}}$ at released $p = 0$ bars directly yields the intrinsic optical anisotropy of a fully detwinned but stress-free material. However, the remanent optical anisotropy decreases with increasing $T$, as thermally assisted domain-wall motion leads to retwinning of the sample as $p$ is released. By 130 and 135 K [Figs. 3(e) and 3(d)], the half-hysteresis loop has essentially collapsed to give zero remanent optical anisotropy at $p = 0$ bars. For $T \geqslant T_s$ the material is tetragonal and no half hysteresis is observed. In this temperature regime the $p$ dependence of $R_{\text{ratio}}(\omega)$ can be described by a linear response [Figs. 1(b) and 3(f)–3(h)].

We return to the $T$ dependence of the remanent anisotropy shortly, after first discussing the results of the PC fixed-$p$ measurements (brown and green stars in Fig. 3), which provide additional insight. Specifically, cooling the specimen across $T_s$ with either $p = 0.3$ or 0.8 bars results in an optical anisotropy that coincides with the upper branch of the half-hysteresis $p$ loops. The same optical anisotropy is indeed obtained whether $p$ is increased to 0.8 bars following a ZPC $p$-loop experiment or the sample is cooled through $T_s$ at constant $p$ (PC measurement). The latter experimental conditions as well as the resulting optical anisotropy are fully equivalent to and in agreement with the experiment and data reported in Refs. [25] and [26]. The results for $p = 0.3$ bars (brown stars in Fig. 3) indicate that this $p$ applied at $T > T_s$ is enough to fully detwin the specimen.

As an additional experimental protocol, we measured $\Delta R_{\text{ratio}}$ for increasing $T$ after first cooling through $T_s$ to 10 K at $p = 0.8$ bars and then releasing the pressure to $p = 0$ bars (solid and open gray stars in Fig. 3). The $T$ dependence of the resulting optical anisotropy upon warming the specimen at $p = 0$ bars [zero pressure warming (ZPW)] consistently coincides with the remanent state of $\Delta R_{\text{ratio}}$, underscoring the analogy to zero-field and field-cooling magnetization measurements of a ferromagnet.

Figure 4(a) summarizes the $T$ dependence of the optical anisotropy $\Delta R_{\text{ratio}}$ for $x = 0$ read at fixed $p$ along the virgin curve of $\Delta R_{\text{ratio}}$ between 0 and 0.8 bars (Fig. 3). For $p \leqslant 0.2$ bars, $\Delta R_{\text{ratio}}$ is almost $T$ independent and weakly negative above $T_s$ [35] and undergoes a sharp onset at $T_s$. For $p > 0.4$ bars $\Delta R_{\text{ratio}}$ is $T$ dependent already above $T_s$, displaying a broad crossover through the structural transition, strikingly similar to the anisotropy observed in the dc resistivity $\Delta\rho/\rho = 2(\rho_b - \rho_a)/(\rho_a + \rho_b)$ [10], shown in the same figure for comparison. $\Delta R_{\text{ratio}}$ increases and then saturates at low $T$. The broadening in the $T$ dependence of $\Delta R_{\text{ratio}}$ for $T > T_s$ is progressively enhanced for larger applied $p$, which acts here as an external symmetry breaking field.

We now turn our attention to the quantity $\Delta R_{\text{ratio}}/p$ which is somewhat analogous to a susceptibility [36]; it relates the

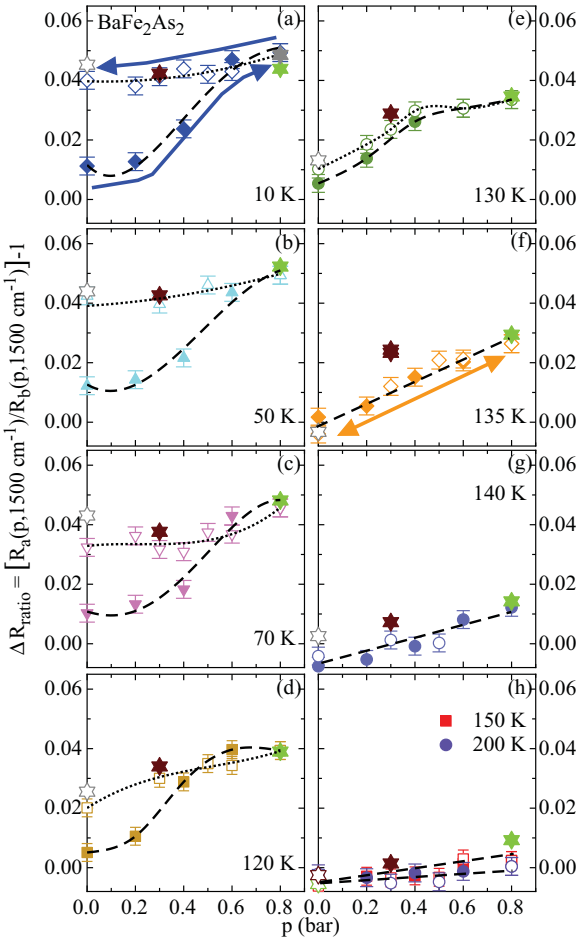


FIG. 3. (Color online) Optical anisotropy ($\Delta R_{\rm ratio}$) of $BaFe_2As_2$ as a function of pressure at representative temperatures: (a)–(h) Solid and open symbols denote increasing and decreasing $p$, respectively, for $p$-loop measurements following an initial ZPC protocol. Our measurements show that in the orthorhombic phase the optical anisotropy exhibits a hysteretic behavior due to twin boundary motion, while in the tetragonal phase a reversible linear response to applied $p$ is recovered [Fig. 1(b)]. Data from PC fixed-$p$ measurements are shown by brown and green stars for $p = 0.3$ and 0.8 bars, respectively. Additional gray stars indicate measurements for which the sample was initially prepared by $p$ cooling to 10 K with $p = 0.8$ bars, at which temperature $p$ was released. The optical anisotropy was then measured as a function of $T$ while warming under conditions of $p = 0$ bars (i.e., PC-ZPW experiment). Dashed and dotted lines are drawn to guide the eye. Arrows [blue in (a) and orange in (f)] sketch the $p$-increasing/decreasing and $p$-sweeping loops at 10 K ($T < T_s$) and 135 K ($T \geqslant T_s$), respectively.

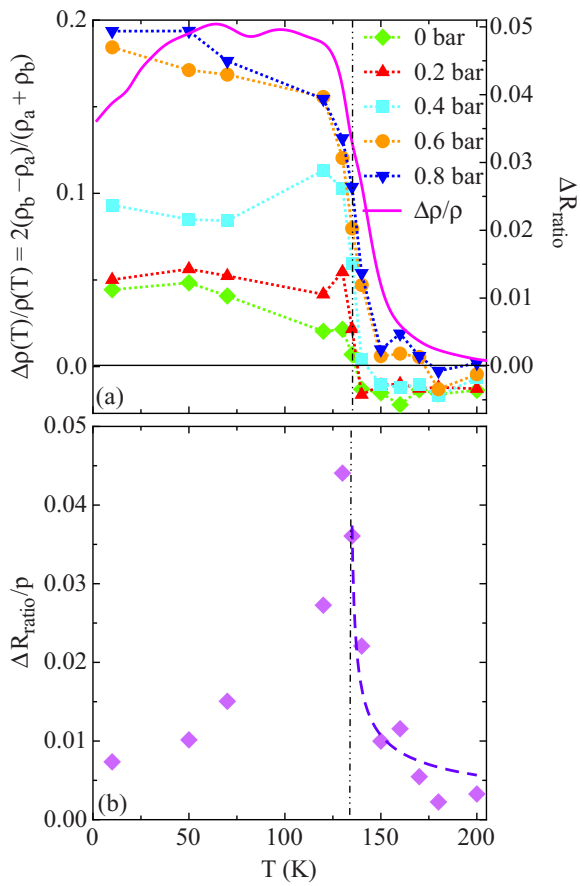


FIG. 4. (Color online) Temperature dependence of the pressure-induced optical anisotropy in $BaFe_2As_2$: (a) $T$ dependence of $\Delta R_{\rm ratio}$ at fixed $p$, from data along the virgin curve (Fig. 3), compared to the dc anisotropy ratio $\Delta\rho/\rho$, obtained from transport results in the case of samples constantly held under uniaxial pressure [10]. The dotted lines are guides to the eyes. (b) $T$ dependence of $\Delta R_{\rm ratio}/p$. The dashed line corresponds to a Curie-like behavior (see text). The vertical double-dotted-dashed line defines the transition temperature $T_s$.

induced optical anisotropy to the applied stress and can be obtained from the linear $p$-dependent behavior of $\Delta R_{\rm ratio}$ for $T \geqslant T_s$ [Figs. 3(f)–3(h)]. At 130 K a linear $p$ dependence of $\Delta R_{\rm ratio}$ is observed only below 0.6 bars, before the saturation sets in. Here we calculate $\Delta R_{\rm ratio}/p$ in the interval 0–0.6 bars. Below 120 K we just consider the slope of $\Delta R_{\rm ratio}(p)$ at the onset of the virgin curve, thus between 0 and 0.2 bars. $\Delta R_{\rm ratio}/p$ as a function of $T$ is shown in Fig. 4(b) and may represent an optical estimate of the susceptibility caused by the fluctuations of the nematic phase. This quantity displays an incipient divergence for $T$ close to $T_s$, rather similar to what has been inferred from dc transport data [11]. If the data for $T > T_s$ are fit to a simple power law, $\Delta R_{\rm ratio}/p \sim (T - T_s)^{-n}$, a best fit value $n \sim 0.5$ is obtained. Deviation from the anticipated mean-field exponent ($n = 1$) possibly reflects uncertainty in the measured anisotropy and the relatively small $T$ grid. Nevertheless, the behavior of $\Delta R_{\rm ratio}/p$ [Fig. 4(b)] indicates a remarkable sensitivity of the electronic structure to applied stress even at the relatively high energies probed by the MIR optical reflectivity. Our observations of $p$-induced optical anisotropy for $T > T_s$ are in broad agreement with ARPES data [22,23] taken for fully detwinned specimens, which reveal a $p$-induced energy splitting of two orthogonal bands with dominant $d_{xz}$ and $d_{yz}$ character already at $T > T_s$. Consistent with previous elastoresistance measurements [11,15] there is no evidence for any divergence of the optical susceptibility at higher temperatures, arguing against the presence of any additional nematic phase transitions at

$T^* > T_s$, as proposed, for instance, by the recent magnetotorque experiment [32].

Our measurements establish important constraints on models that aim to describe the nematic phase transition in underdoped Fe-arsenide superconductors. The large anisotropy in the optical reflectivity observed in the tetragonal state for applied uniaxial stress implies an important role for the orbital degrees of freedom [3–9], affecting the band structure far from the Fermi energy. Although these measurements alone cannot distinguish the driving force behind the nematic order, scenarios for the structural and magnetic transitions that are generally based on the involvement of spin-orbital coupling set the stage for the emergence of high-temperature superconductivity in the iron-pnictides. Furthermore, we establish that a relatively modest stress is able to fully detwin the material in the orthorhombic phase. While a complete analysis of the energetics of domain-wall motion is beyond the scope of this Rapid Communication, these data (together with recent measurements of field-induced detwinning [37]) motivate a careful theoretical investigation of the interplay of nematic order and the coupled structural deformation at twin boundaries. Finally, we remark that the experimental tools that we have developed to study the strain-induced anisotropy in the dc resistivity [15] and optical reflectivity (this work) open an avenue for the study of incipient nematic order in strongly correlated materials.

The authors wish to thank A. Lucarelli for his initial contribution in designing the pressure device and R. Fernandes, A. Chubukov, W. Ku, M. Sigrist, S. Kivelson, M. Dressel, D. N. Basov, and D. Lu for fruitful discussions. This work was supported by the Swiss National Foundation for the Scientific Research within the NCCR MaNEP pool. Work at Stanford University was supported by the Department of Energy, Office of Basic Energy Sciences under Contract No. DE-AC02-76SF00515.

[1] I. R. Fisher *et al.*, Rep. Prog. Phys. **74**, 124506 (2011), and references therein.
[2] M. A. Tanatar *et al.*, Phys. Rev. B **79**, 180508(R) (2009).
[3] C.-C. Lee *et al.*, Phys. Rev. Lett. **103**, 267001 (2009).
[4] C.-C. Chen *et al.*, Phys. Rev. B **82**, 100504(R) (2010).
[5] W. Lv *et al.*, Phys. Rev. B **82**, 045125 (2010).
[6] C. Fang *et al.*, Phys. Rev. B **77**, 224509 (2008).
[7] C. Xu *et al.*, Phys. Rev. B **78**, 020501(R) (2008).
[8] R. M. Fernandes *et al.*, Phys. Rev. B **85**, 024534 (2012).
[9] S. Avci *et al.*, arXiv:1303.2647.
[10] J.-H. Chu *et al.*, Science **329**, 824 (2010).
[11] J.-H. Chu *et al.*, Science **337**, 710 (2012).
[12] A. F. Wang *et al.*, New J. Phys. **15**, 043048 (2013).
[13] J. J. Ying *et al.*, Phys. Rev. Lett. **107**, 067001 (2011).
[14] E. C. Blomberg *et al.*, Nat. Commun. **4**, 1914 (2013).
[15] H.-H. Kuo *et al.*, Phys. Rev. B **88**, 085113 (2013).
[16] S. Jiang *et al.*, Phys. Rev. Lett. **110**, 067001 (2013).
[17] R. M. Fernandes *et al.*, Phys. Rev. Lett. **105**, 157003 (2010).
[18] A. E. Böhmer *et al.*, Phys. Rev. Lett. **112**, 047001 (2014).
[19] C. Dhital *et al.*, Phys. Rev. Lett. **108**, 087001 (2012).
[20] L. W. Harriger *et al.*, Phys. Rev. B **84**, 054544 (2011).
[21] Y. Song *et al.*, Phys. Rev. B **87**, 184511 (2013).
[22] M. Yi *et al.*, Proc. Natl. Acad. Sci. USA **108**, 6878 (2011).
[23] M. Yi *et al.*, New. J. Phys. **14**, 073019 (2012).
[24] Q. Wang *et al.*, arXiv:1009.0271.
[25] A. Dusza *et al.*, Europhys. Lett. **93**, 37002 (2011).
[26] A. Dusza *et al.*, New J. Phys. **14**, 023020 (2012).
[27] M. Nakajima *et al.*, Proc. Natl. Acad. Sci. USA **108**, 12238 (2011).
[28] M. Nakajima *et al.*, Phys. Rev. Lett. **109**, 217003 (2012).
[29] Y. Gallais *et al.*, Phys. Rev. Lett. **111**, 267001 (2013).
[30] T.-M. Chuang *et al.*, Science **327**, 181 (2010).
[31] M. P. Allan *et al.*, Nat. Phys. **9**, 220 (2013).
[32] S. Kasahara *et al.*, Nature (London) **486**, 382 (2012).
[33] See Supplemental Material at http://link.aps.org/supplemental/10.1103/PhysRevB.89.060501 for further details of the samples preparation and experimental technique as well as additional experimental protocols.
[34] Each experimental protocol was repeated over several runs for each combination of $T$ and $p$. Therefore, $\Delta R_{\rm ratio}$, representing the optical anisotropy and shown in Fig. 3, was obtained as an average of equivalent experiments.
[35] A change of sign of the optical anisotropy, defined as dichroism, for $x = 0$ when crossing the structural transition at $T_s$, was already identified in earlier experiments at fixed applied pressure [25, 26]. It has been proposed that the onset of orbital ordering at the coincident structural and magnetic transition may lead to changes of the sign as well as of the intensity of the dichroism [4]. The small optical anisotropy obtained for $p \sim 0$ bars at $T < T_s$ following a ZPC protocol implies the presence of weak residual strains in the crystal.
[36] Following the detailed discussion in Refs. [11] and [15], strain ($\epsilon$) acts as a field on the nematic order parameter ($\psi$). Hence, the nematic susceptibility is defined as $\partial\psi/\partial\epsilon$. In a mean-field analysis, this quantity diverges following a Curie-Weiss temperature dependence, with a Weiss temperature below the actual structural transition temperature $T_s$. In contrast, the quantity $\partial\psi/\partial p$ differs from the actual nematic susceptibility since it involves the elastic compliance of the crystal lattice, and in a mean-field analysis diverges following a Curie-Weiss temperature dependence with a Weiss temperature equal to $T_s$.
[37] J. P. C. Ruff *et al.*, Phys. Rev. Lett. **109**, 027004 (2012).